Atmospheric Environment 55 (2012) 311–318

Contents lists available at SciVerse ScienceDirect

Atmospheric Environment

journal homepage: www.elsevier.com/locate/atmosenv

Characterization of PM-PEMS for in-use measurements conducted during validation testing for the PM-PEMS measurement allowance program

M. Yusuf Khan [a], Kent C. Johnson [a,*], Thomas D. Durbin [a], Heejung Jung [a], David R. Cocker III [a], Dipak Bishnu [b], Robert Giannelli [c]

[a] University of California, College of Engineering, Center for Environmental Research and Technology (CE-CERT), Riverside, CA 92507, USA
[b] California Air Resources Board (CARB), 1001 I Street, Sacramento, CA 95814, USA
[c] US Environmental Protection Agency (EPA), 2000 Traverwood Dr., Ann Arbor, MI 48105, USA

ARTICLE INFO

Article history:
Received 30 September 2011
Received in revised form
29 February 2012
Accepted 2 March 2012

Keywords:
PM-PEMS
Diesel particulate matter
Quartz crystal microbalance
Photo-acoustic
Regeneration
Non-regeneration
Size distribution

ABSTRACT

This study provides an evaluation of the latest Particulate Matter-Portable Emissions Measurement Systems (PM-PEMS) under different environmental and in-use conditions. It characterizes four PM measurement systems based on different measurement principles. At least three different units were tested for each PM-PEMS to account for variability. These PM-PEMS were compared with a UC Riverside's mobile reference laboratory (MEL). PM measurements were made from a class 8 truck with a 2008 Cummins diesel engine with a diesel particulate filter (DPF). A bypass around the DPF was installed in the exhaust to achieve a brake specific PM (bsPM) emissions level of 25 mg $hp^{-1}h^{-1}$. PM was dominated by elemental carbon (EC) during non-regeneration conditions and by hydrated sulfate ($H_2SO_4.6H_2O$) during regeneration. The photo-acoustic PM-PEMS performed best, with a linear regression slope of 0.90 and R^2 of 0.88 during non-regenerative conditions. With the addition of a filter, the photo-acoustic PM-PEMS slightly over reported than the total PM mass (slope = 1.10, R^2 = 0.87). Under these same non-regeneration conditions, a PM-PEMS equipped with a quartz crystal microbalance (QCM) technology performed the poorest, and had a slope of 0.22 and R^2 of 0.13. Re-tests performed on upgraded QCM PM-PEMS showed a better slope (0.66), and a higher R^2 of 0.25. In the case of DPF regeneration, all PM-PEMS performed poorly, with the best having a slope of 0.20 and R^2 of 0.78. Particle size distributions (PSD) showed nucleation during regeneration, with a shift of particle size to smaller diameters (~64 nm to ~13 nm) with elevated number concentrations when compared to non-regeneration conditions.

1. Introduction

Particulate matter (PM) is known for its potential to cause health problems. Regulatory agencies around the world are targeting in-use gaseous and PM emissions to ensure low emissions levels are maintained throughout the course of the engine's lifetime in real world driving conditions. In the United States (US), measurements of in-use emissions are required for regulatory purposes within a defined portion of the engine map known as Not-To-Exceed (NTE) control area. These measurements are made with Particulate Matter-Portable Emissions Measurement Systems (PM-PEMS) that are specifically developed to measure and quantify PM emissions on a mass basis under the protocols specified in the regulations.

PM is a complex mixture of extremely small particles and liquid droplets. It mainly consists of elemental and organic carbon (EC/OC), absorbed hydrocarbons and inorganic compounds (sulfate, water, etc.). There are numerous technologies by which PM mass can be quantified. These technologies utilize different measuring principles, such as a quartz crystal microbalance (QCM), photo-acoustic (PA) detection, combined mobility and inertial sizing, laser-induced incandescence (LII), light scattering (LS), combined diffusion charging and gravimetric filter, and photoelectrical charging (Baron and Willeke, 2001; Mohr et al., 2005).

There have been numerous studies quantifying PM mass using available technologies and comparing them with the gravimetric method. These technologies have been evolving over the last decade. For in-use compliance testing, QCM and PA methods have both been developed and evaluated. Booker et al. (2007) evaluated QCM technology on a prototype unit and found a good correlation with a non-portable (constant volume sampling) certification

* Corresponding author.
E-mail address: kjohnson@cert.ucr.edu (K.C. Johnson).

1352-2310/$ – see front matter © 2012 Elsevier Ltd. All rights reserved.
doi:10.1016/j.atmosenv.2012.03.004

system. In an on-road study with a pre-commercial PEMS with QCM technology, however, Johnson et al. (2011) showed a positive or negative measurement bias, depending upon the PM mass composition. In earlier studies of the PA measurement method, Schindler et al. (2004) showed an excellent correlation, R^2 >0.95, with black carbon on a gravimetric filter. Conversely, in a recent chassis dynamometer tests, Durbin et al. (2007) found 13–22% lower PM mass for a pre-commercial PA PEMS when compared to gravimetric filter mass. Another pre-commercial PM-PEMS using a combination of diffusion charging and a gravimetric filter showed positively biased results with a poor coefficient of determination, R^2 = 0.55, during preliminary in-use testing program (Johnson et al., 2011). Other technologies that have been evaluated and compared to PM mass (LII, LS, combined diffusion charging and gravimetric filter, combined mobility and inertial sizing, photoelectric charging, etc.) have shown mixed results in such comparisons, with some showing good correlations (Lehmann et al., 2004; Maricq et al., 2006; Matter et al., 1999; Podsiadlik et al., 2003; Witze et al., 2004), while other instruments have shown poor correlations (Johnson et al., 2011; Durbin et al., 2007). Overall, the behavior for this full range of PM measurement technologies is not fully understood and needs to be explored to better understand the sensitivity of these instruments at lower levels of PM, their reproducibility, and their linearity with the gravimetric filter method.

The measurement of PM mass under in-use driving conditions is complex and has higher uncertainty in comparison to laboratory measurements. Therefore, it is important to characterize and quantify difficulties in making these measurements with PEMS. The US Environmental Protection Agency (EPA), the California Air Resources Board (CARB) and the Engine Manufacturers Association (EMA) formed a measurement allowance steering committee (MASC) to develop a program to account for uncertainties in PM-PEMS measurements. These uncertainties were subsequently accounted for in regulations relating to in-use emissions measurements via a measurement allowance (MA). The MASC approach for the PM measurement allowance was similar to that used for the gas phase program (Johnson et al., 2009). This included laboratory testing and Monte Carlo modeling at Southwest Research Institute (SwRI), followed by in-use testing using the University of California at Riverside's (UCR) Mobile Emission Laboratory (Johnson et al., 2010).

This study describes the in-use characterization of the PM-PEMS as part of the PM MA program. A series of tests were performed, specifically designed to quantify the performance of commercially available PM-PEMS and to determine their validity as PM measurement systems for regulatory use. In comparison with previous studies of PM-PEMS (Johnson et al., 2011), this study provides the latest evaluation of PM-PEMS as the technology stands at the start of the in-use compliance testing program. Unique to this study was that several PM-PEMS with multiple serial numbers were evaluated over a repeatable series of different on-road driving conditions with variations in environmental conditions and elevations. Approximately 100 tests were performed for each unit to statistically quantify differences between like models. Additionally one PM-PEMS was upgraded during this research and retested, where it showed significant improvements. The MEL provided a unique testing platform in that it contains a full 1065-compliant constant volume sampling (CVS) system with gravimetric PM measurements, while being fully operational under on-road driving conditions (Cocker et al., 2004a and 2004b). Measurements were made from a 2009 class 8 heavy-duty diesel vehicle, equipped with an original equipment manufacturer (OEM) Diesel Particulate Filter (DPF) with a bypass to simulate a cracked DPF. This study focused on PM emission levels targeted at 0.025 g $hp^{-1}h^{-1}$, which is at the regulatory limit during non-regeneration conditions and close to the heavy-duty on board diagnostics (HD-OBD) PM threshold, which is currently set at 0.07, but will eventually be reduced to 0.03 g $hp^{-1}h^{-1}$ for model year 2016 and later (CARB, 2010). In addition to this study, PM-PEMS were also evaluated during regeneration-only conditions. This study represents the most comprehensive and definitive evaluation of current, regulatory compliant, PM-PEMS technologies that are commercially available for use under in-use operating conditions.

Table 1
Test matrix for PM-PEMS in-use evaluations.

PM-PEMS ID	Manufacture	Product name	Principle of detection	In-use testing
PEMS1(DC + F)	Horiba	TRPM	Diffusion charging + gravimetric filter	No
PEMS2(QCM)1,2,3	Sensors Inc	PPMD	Quartz crystal microbalance	Yes
PEMS3(PA)1,2,3,4	AVL	MSS 483	Photo-acoustic	Yes
PEMS3(PA + F) 1,2,3,4	AVL	MSS 483 + GFM	Photo-acoustic + gravimetric filter	Yes[a]
INST4(LS)	TSI	DustTrak 8530	90° light scattering	Yes
INST5(EM + A)	Dekati	DMM	Electrical mobility + aerodynamic impaction	Yes

[a] Although the AVL's MSS 483 GFM was tested where only one serial number conditioning unit and filter module were evaluated, but three different serial number MSS 483's were tested.

2. Experimental methods

2.1. Test vehicle

Measurements were made from a 2009 class 8 truck equipped with a 2008 Cummins 15 L heavy-duty diesel engine. The engine was equipped with a DPF, and was certified to meet the 0.01 g $hp^{-1}h^{-1}$ PM standard. The vehicle was selected to represent a heavy-duty diesel vehicle with DPF-out bsPM emissions of approximately 0.001 g $hp^{-1}h^{-1}$. The MEL provided the load for the testing, with a combined weight of the tractor and trailer of 65,000 lbs. The vehicle odometer reading was 64,000 miles at the beginning of the study. A bypass system was set-up for the after-treatment system (ATS), designed to simulate a cracked DPF but with a properly functioning diesel oxidation catalyst (DOC). The bypass included a DOC and was successful in meeting the targeted bsPM emissions level of 25 mg $hp^{-1}h^{-1}$ (0.025 g $hp^{-1}h^{-1}$) for non-regeneration conditions in both the validation and re-test phases. The bypass system was not used during regeneration, where accumulated soot was removed from the DPF.

2.2. PM-PEMS description

Overall, four PM measurement systems were used for this study (Table 1). The nomenclature used for these PM measuring systems distinguishes them on the basis of their ability to report mass emissions, as opposed to measuring concentrations, and the measurement principle used. Systems that are capable of providing bsPM measurements and that meet the criteria defined for PEMS for in-use compliance testing under 40 CFR Part 1065 regulations are called PEMS. Systems that are only designed to provide PM mass concentration in the exhaust are called instruments, or INST. The two types of PM-PEMS systems that were tested in this study are denoted as PEMS2(QCM) and PEMS3(PA). At least three different units of PEMS2(QCM) and PEMS3(PA) were tested. These units are denoted as 1, 2, 3 and 4 in Table 1. By testing different

units, the consistency of the measurement principle and instrument design can be evaluated. The other two PM systems that were utilized in this study are referred as INST4(LS) and INST5(EM + A). These instruments are already integrated into the MEL. Another PEMS, PEMS1(DC + F), was evaluated for possible inclusion in this study, but it was not included on the basis of preliminary testing results from SwRI.

The PEMS2(QCM) system is Sensor's Portable Particulate Mass Device (PPMD). The PPMD measurement principle is based on the QCM technology that employs piezoelectric crystals. Particles in the exhaust are deposited on the crystal surfaces after being charged. The total mass deposited is calculated from the change in frequency of the oscillating crystal due to deposited PM mass. This technology has the potential to quantify all types of PM, although there has been some concern related to the sensitivity of the instrument, and the possible need for crystal greasing to help the particles stick to the surface of the crystal (Johnson et al., 2010, 2011).

The PEMS3(PA) system is AVL's Micro Soot Sensor (MSS) model 483. This PM-PEMS is based on a photo-acoustic light absorption sensing principle. It measures a periodic pressure wave caused by the absorption of a modulated IR laser beam by particles, and the resulting periodic heating and cooling of the exhaust gas. The resulting periodic pressure wave is recorded by a microphone, and it's amplitude is enhanced using a resonant acoustic cell. This system is specially designed for soot, and therefore, performs well for soot dominated PM (Bell and Phil, 1881; Harren et al., 2000; Schindler et al., 2004) and poor for the organic and inorganic fraction of PM (Johnson et al., 2011). In an effort to characterize total PM mass, the PEMS3(PA) manufacturer upgraded their soot measurement with a prototype Gravimetric Filter Module (GFM) to enhance their measurement approach with a gravimetric filter that essentially calibrates the PA signal to a gravimetric mass. This prototype module was not used in the preliminary laboratory testing at SwRI. In this study, the MSS unit with the addition of GFM is denoted as PEMS3(PA + F).

INST4(LS) is TSI's DustTrak 8520. This PM system utilizes an optical light scattering measurement technique that is strongly influenced by particle size (Durbin et al., 2007; Hinds, 1998). The light emitted from the laser diode is scattered by particles, and the amount of light scatter determines the particle mass concentration. The total amount of light emitted from the laser diode that is scattered by particles determines the particle mass concentration based on a calibration factor. ISNT4(LS) was calibrated to diesel exhaust using measurements by the MEL back in 2005 (Durbin et al., 2007).

INST5(EM + A) is a DMM 230 that combines different aerosol measurement principles: electrical charging and detection, and aerodynamic inertial impaction (Ristimaki et al., 2002). The particle stream is charged by a corona discharger, and the electrical mobility of the particles is used to detect particles below 30 nm. Inertial size separation is done in a six stage low pressure cascade impactor to estimate the mass concentration of particle sizes ranging from 30 nm to 532 nm.

2.3. PEMS installation and operation

PEMS2(QCM) and PEMS3(PA) were mounted on a frame installed on the tractor for all the in-use testing, while INST4(LS) and INST5(EM + A) were mounted within the MEL. INST4(LS) and INST5(EM + A) sampled from the MEL's CVS. The operation for all PM systems was performed according to the manufacturer's specifications. It should be noted that PEMS2(QCM) was re-tested after the manufacturer upgraded the system. The PEMS2(QCM) was upgraded for the re-tests with higher sensitivity and improved crystal burn-in procedures to allow for higher loadings, which reduced the need to reuse crystals.

2.4. MEL operation

The MEL's primary tunnel flow rate was set to 2700 standard cubic feet per minute (scfm) and the secondary tunnel was set to provide a secondary dilution of 2.27:1. These dilution conditions created a CVS sample temperature that averaged 80 °C, with a single standard deviation of 20 °C throughout the test program.

2.5. MEL PM measurements

PM mass concentrations were determined gravimetrically on pre-weighed 47 mm diameter 2- μm pore Teflo® filters (Whatman). Loaded Teflo® filters were weighed using a Mettler Toledo UMX2 microbalance following the guidelines within the Code of Federal Regulations (CFR, 2010). Teflo® filters were subsequently extracted with High Performance Liquid Chromatography (HPLC) grade water and isopropyl alcohol, and analyzed for sulfate ions using a Dionex DX-120 ion chromatograph. Sulfate PM on the Teflo® filter was assumed to be in hydrated form ($H_2SO_4.6H_2O$), as predicted using the aerosol thermodynamic model ISORROPIA (Nenes et al., 1998; Fountoukis and Nenes, 2007; ISORROPIA, 2009). Parallel 2500 QAT-UP Tissuquartz Pall (Ann Arbor, MI) 47 mm filters (preconditioned at 600 °C for a minimum of 5 h) were used to collect PM for subsequent elemental and organic carbon (EC/OC) analysis following the NIOSH (Manual of Analytical Methods, 1996) method using a Sunset Laboratory (Forest Grove, OR) thermal/optical carbon aerosol analyzer. Particle size distributions were measured using a fast Scanning Mobility Particle Sizer (fSMPS). During this test program, the fSMPS was operated in the size range of 8–188 nm with a 5 s scan time, compared to the 60–90 s for a more traditional SMPS (Shah and Cocker, 2005). A TSI condensation particle counter (CPC) 3760 was used to count the particle number.

2.6. Calculation method

Three different calculation methods are allowed in 40 CFR Part 1065 to determine in-use brake specific PM emissions. In this study, the method 2 calculation from the PM MA was applied to calculate emission factors. The method 2 calculation adjusts the exhaust flow measurement by a ratio of the CO_2-based fuel flow to the ECM reported fuel flow. This method is presented in its simple form in Equation (1), and with the full formula details in Khalek et al. (2010).

$$\text{Method 2} = \frac{\sum g}{\sum\left[\frac{\text{Carbon}_{\text{fuel}}}{\text{ECM}_{\text{fuel}}} \times \text{Work}\right]} \quad (1)$$

2.7. Reference accuracy

Prior to the in-use testing, the MEL was cross compared with SwRI at an emission level of 0.025 g $hp^{-1}h^{-1}$ for PM was subjected to a 1065 audit. The MEL was, on average, lower than SwRI by about 6% on a simulated NTE transient cycle (Johnson et al., 2010). Some of this difference could be attributed to line losses, since the sample transfer line from the engine cell to the MEL was longer than the transfer line used in the engine cell itself. The 6% difference is well within the measurement variability of other round robin studies (Traver, 2002), and suggests the MEL is a reasonable reference tool for comparing PM-PEMS in-use and for quantifying in-use uncertainties (Johnson et al., 2011).

2.8. Test routes

The in-use routes were designed to be similar to those used in a previous PM-PEMS study (Johnson et al., 2011) to provide a range of environmental conditions, and included segments near sea level, in coastal regions, and in desert regions, and with longer uphill incline segments and segments at elevations up to 1500 m. Over the different courses, the temperatures varied from 10 to 43 °C, several large power line transmissions were crossed providing potential electromagnetic interference (EMI), and several railroad track crossings and pot holes provided vibration disturbances.

3. In-use PM results

This section includes results from the comparison of PM systems with MEL reference method, and results for PM composition and particle size distributions (PSD). During testing, the MEL demonstrated a carbon balance within 2% and a high R^2 of 0.98, thus suggesting the data provided in this research is of high quality, see (Johnson et al., 2010) for more information.

3.1. PM analysis basis

The PM analysis was done on a brake specific basis for the in-use testing. Only PM emissions measured within the NTE work zone, as mentioned earlier, were used for this comparison. The NTE work zone excludes operation when the engine is at low loads, a condition where the brake specific emissions are exaggerated by low values of the work term. The results presented in this study are based on a subset of the actual data sampled due to data yield from issues found during testing and post processing.

3.2. PEMS bsPM results

Comparisons between the PEMS and the gravimetric PM measurements of the MEL were made using correlations to evaluate the bias of the different systems. A summary of the results of this correlation analysis is provided for individual units (Table 2) and for the combined results for all units (Table 3).

3.2.1. PEMS2(QCM) bsPM

The correlations between PEMS2(QCM) and the MEL are shown in Fig. 1. The correlations for all units of PEMS2(QCM) were poor. The overall correlation for non-regeneration tests showed an $R^2 = 0.13$, a slope of 0.22, and a positive intercept of 4.3 mg $hp^{-1}h^{-1}$. In moving from unit 1 to unit 3, both the slope (0.26–0.14) and R^2 (0.24–0.04) decreased. The PM concentration increased for the testing going from unit 1 to unit 3 in an effort to reduce sample times, which may be one of the factors contributing to the decreasing correlation going from unit 1 to unit 3 (Johnson et al., 2010). Unit 3 also had a large zero intercept at 7.7 mg $hp^{-1}h^{-1}$, which may be a result of changing its crystal usage logic (Johnson et al., 2010). The PEMS2(QCM) non-regeneration mean bias at the 20 mg $hp^{-1}h^{-1}$ bsPM emissions was −10 mg $hp^{-1}h^{-1}$, and at 30 mg $hp^{-1}h^{-1}$ (i.e., the 2016 OBD threshold) the mean bias was −18 mg $hp^{-1}h^{-1}$. The standard error estimate (SEE) between PEMS2(QCM) and the MEL was relatively high (5.2 mg $hp^{-1}h^{-1}$). The two-tailed, paired *t*-test between the PEMS and MEL bsPM correlations suggests the mean differences were statistically significant at greater than a 99% confidence level, even though the SEE was relatively high. The PEMS2(QCM) regeneration results also showed a low overall correlation with an $R^2 = 0.36$ and a slope of 0.08 (Table 3).

Table 3
PEMS PM bsPM correlation results combined (mg $hp^{-1}h^{-1}$).

PEMS	Slope	Intercept	R^2	SEE	*t*-test
Non-Regeneration Conditions					
PEMS2(QCM)	0.22	4.3	0.13	5.2	3E-65
PEMS3(PA)	0.90	−0.8	0.88	2.9	4E-54
PEMS3(PA + F)	1.10	−1.2	0.87	3.6	4E-54
INST4(LS)	0.76	−1.0	0.74	4.3	1E-96
INST5(EM + A)	0.59	−1.3	0.32	8.3	1E-78
PEMS2(QCM)_UPGRADE	0.66	5.1	0.25	6.8	3E-03
Regeneration Conditions					
PEMS2(QCM)	0.08	2.82	0.36	2.05	2E-03
PEMS3(PA)	−0.01	0.49	−0.68	0.09	1E-03
PEMS3(PA + F)	−0.04	7.38	−0.12	3.52	8E-02
INST4(LS)	−0.06	1.43	−0.24	2.03	1E-05
INST5(EM + A)	0.20	−0.36	0.78	1.44	9E-06

The PEMS2(QCM) system was upgraded to reduce the negative bias and large data spread. For details on the upgrades see (Johnson et al., 2010). The PEMS2(QCM)_UPGRADE also showed a negative bias relative to the MEL, with a correlation slope of 0.84 when forced through zero, and 0.66 when not forced through zero. The intercept was 5.1 mg $hp^{-1}h^{-1}$ with an R^2 of 0.25. The slope increased for the re-test, suggesting better accuracy with the upgraded unit. The R^2 and SEE were about the same for both studies, suggesting the precision did not change significantly between the two studies.

Previous studies with the same MEL showed that the PEMS2(QCM) was overestimating PM compared to the reference method with a slope of 1.5 (Johnson et al., 2011). The composition was based on a similar PM composition, but with higher bsPM emissions. The change in response for PEMS2(QCM) from 1.5 to 0.22 suggests that revisions and upgrades can have a significant effect on the instruments behavior. Part of the reason for the change in response could be from configuring the PEMS for different concentrations levels, as described in Johnson et al. (2010).

3.2.2. PEMS3(PA) bsPM

The correlation plots for the different units of PEMS3(PA) are provided in Fig. 2. The overall correlation for PEMS3(PA) showed an $R^2 = 0.88$, a slope of 0.90, and a negative intercept of 0.8 mg $hp^{-1}h^{-1}$ for non-regeneration tests. The slope and R^2 were relatively consistent between unit 2 through unit 4, where the slope varied from 0.95 to 0.83 and the R^2 varied from 0.86 to 0.95. The PEMS3(PA) non-regeneration mean bias at the 20 mg $hp^{-1}h^{-1}$ bsPM emissions was −2.8 mg $hp^{-1}h^{-1}$, and at 30 mg $hp^{-1}h^{-1}$ the

Table 2
Non-regeneration PEMS bsPM correlation by unit 1,2,3 and 4 (mg $hp^{-1}h^{-1}$).

PEMS	Slope				Intercept				R^2			
	1	2	3	4	1	2	3	4	1	2	3	4
PEMS2(QCM)	0.26	0.25	0.14		2.3	3.0	7.7		0.24	0.13	0.04	
PEMS3(PA)		0.95	0.83	0.86		−1.0	−0.4	−0.4		0.86	0.93	0.95
PEMS3(PA + F)		1.16	1.01	1.07		−1.4	−0.3	−0.9		0.86	0.89	0.95
INST4(LS)	1.00	0.70	0.74	0.76	−3.4	−0.7	−1.1	−0.7	0.80	0.75	0.81	0.79
INST5(EM + A)	1.32	0.39	0.37	0.81	−9.0	0.4	2.8	−5.2	0.56	0.57	0.50	0.73

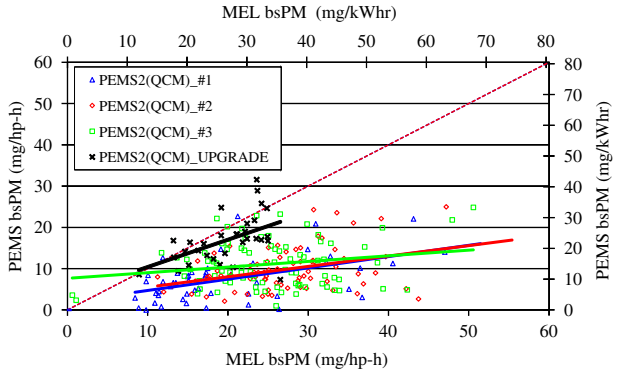

Fig. 1. PEMS2(QCM) non-regeneration bsPM correlation unit by unit.

mean bias was −3.8 mg $hp^{-1}h^{-1}$, or 13% of the OBD threshold. The SEE between the PEMS3(PA) and the MEL was relatively low at 2.9 mg $hp^{-1}h^{-1}$. The two-tailed, paired *t*-test between the PEMS3(PA) and MEL bsPM correlation results suggests the mean differences were statistically significant at a greater than 99% confidence level.

The PEMS3(PA) system showed a very similar correlation compared to a previous study, where the slope averaged 0.91 and the R^2 was 0.95 (Johnson et al., 2011). Between the previous study and this study, four units have been tested with the same MEL where the slope and R^2 were relatively similar, thus suggesting this PEMS measurement technology is mature and reliable.

The PEMS3(PA) regeneration results showed a low overall correlation, with an $R^2 = -0.68$ and a slope of −0.01. The negative slope and R^2 suggests there was no correlation between the reference measurement and the PEMS3(PA) measurement. The PEMS3(PA) regeneration results were also poor during the previous work by Johnson et al. (2011).

PEMS3(PA) was upgraded with a prototype gravimetric filter system at the beginning of this research, and is denoted PESM3(PA + F), as discussed earlier. The PEMS3(PA + F) results showed a slope and R^2 of 1.1 and 0.87, respectively, for the non-regeneration conditions. This was the only PEMS during this current evaluation to show a slope greater than one. The PEMS3(PA + F) reduced the mean bias to 6% of the OBD threshold on an absolute basis. The PEMS3(PA + F) regeneration evaluation still showed a negative slope and a poor R^2 suggesting the gravimetric filter compensation system does not work for all PM compositions.

Further analysis of the PEMS3(PA + F) gravimetric filter showed that the PEMS system did not capture the same mass as the reference filter, with the PEMS filter showing only trace amounts of sulfuric acid PM (<10 μg) while the reference system had in excess of 1000 μg for a comparable sample duration. This suggests a possible particle dilution/formation issue with the PEMS micro-dilution system, which has much lower flow rates and a higher surface area to volume ratio compared to the reference system. The PEMS2(QCM) system also uses a similar dilution process, and had issues with a low response or non-detection for nano-sized sulfuric acid particles, as discussed by Johnson et al. (2011). Additional studies are needed to understand the reason for the PEMS2(QCM) and PEMS3(PA + F) low response for regeneration conditions.

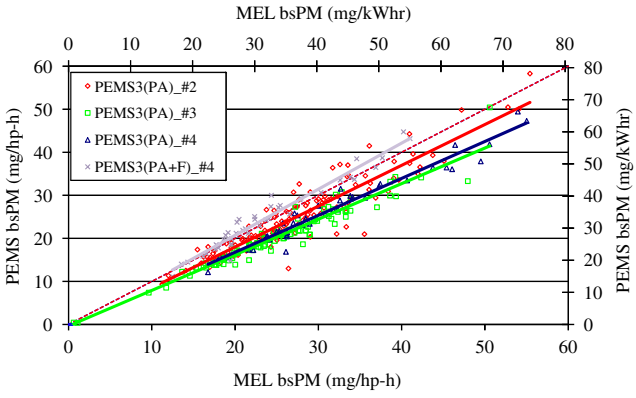

Fig. 2. PEMS3(PA) non-regeneration bsPM correlation unit by unit. PEMS3(PA + F) is added to compare unit 4 against PEMS3(PA).

One of the PEMS3(PA + F) events had a dominant fraction of organic PM. The agreement with the reference system for this case could be improved for PEMS3(PA + F) by using a model-based approach. This approach was based on a model developed by Clerc and Johnson (1982) that uses a combination of hydrocarbon levels, catalyst loading, fuel sulfur levels and ATS temperature to help estimate the amount of material that condenses on a particle surface during dilution. Using this model, the agreement between PEMS3 and the reference method was improved from 55 to 60% negative bias to a 10% negative bias. Further development of models to account for the dynamics of dilution processes could help improve filter-based PM-PEMS that are used for generalized in-use PM inventories and models.

3.2.3. *INST4(LS) & INST5(EM + A)*

INST4(LS) showed a reasonable correlation of $R^2 = 0.74$, a slope 0.76 (Table 3), and a negative intercept of −1 g $hp^{-1}h^{-1}$ for the non-regeneration PM tests. However, there was no correlation for regeneration conditions with a negative R^2 of 0.24. The good correlation for the non-regeneration events suggests this instrument has some correlation with the MEL reference method for the PM composition and size distribution for the non-regeneration, bypassed PM. However, the instrument does not correlate with the gravimetric reference system for regeneration type PM, as has been reported in other studies (Johnson et al., 2011). It should be noted that the good correlation of INST4(LS) with the MEL for non-regeneration can probably be attributed to the previous calibration to the MEL PM mass back in 2005.

INST5(EM + A) showed a lower correlation of $R^2 = 0.32$ and a slope 0.59 (Table 3) compared to INST4(LS) for the non-regeneration tests. This is somewhat surprising since the INST5(EM + A) detection method is more sophisticated than that for INT4(LS) and should detect a wider range of particles with different compositions and particle size distributions. In the case of regeneration tests, INST5(EM + A) performed best relative to all PEMS with a slope of 0.20 and $R^2 = 0.78$. INST4(LS) and INST5(EM + A) showed a lower slope and R^2 in this study compared to the previous study (Johnson et al., 2011). This suggests INST4(LS) and INST5(EM + A) measurement system may be affected by the change the PM emission level.

3.2.4. *Overall PM-PEMS performance*

Results for the combined data sets for all PEMS and INSTs are presented in Fig. 3. All PEMS and INSTs, except for the upgraded PEMS3(PA + F), showed a negative bsPM bias relative to the MEL reference method for both the non-regeneration and regeneration cases. PEMS3(PA) showed the best overall correlation and PEMS2(QCM) the lowest overall correlation, with the correlations for INST4(LS) and INST5(EM + A) in-between those units. PEMS2(QCM) also showed the highest positive zero intercept, while the other PEMS showed slightly negative zero intercepts. PEMS2(QCM)_UPGRADE improved its correlation with the MEL, although precision did not change significantly, as shown in Table 3.

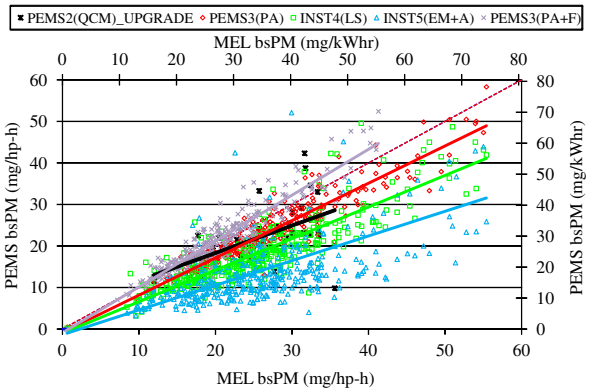

Fig. 3. PEMS and INST non-regeneration bsPM correlation combined.

The performance of the PEMS was also evaluated in terms of their operational characteristics, ease of use, and failures. The PEMS problems ranged from issues related to testing under in-use conditions, operational issues, and post processing issues. The in-use issues ranged from electrical and mechanical connections, crystal usage for short NTE's, valve switching, measurement signals, and crystal behaviors. Operational problems occurred during startup, commissioning, and with the systems prior to testing in-use. Typical issues included incorrect system configurations, procedures that didn't work, and issues with the startup software and other recommended practices that didn't function as discussed in manual. The post processing issues included data filtering, bsPM differences between processor versions, data identification, and calculation methods not being available. The impact of these errors on the results was a factor of approximately 1.3–1.5, depending on the PEMS and the unit number. All of these issues are discussed in detail elsewhere (Johnson et al., 2010). Both the PEMS2(QCM) and PEMS3(PA) had issues that impacted their respective data yields. The PEMS2(QCM) had more issues overall, with data yield of 61% out of 347 valid events. The PEMS3(PA) had fewer issues, with an average data yield of 70%. This data yield was impacted by unit 1, which had a low yield of 15% due to the prototype gravimetric filter module and not the PEMS3(PA) system. PEMS3(PA) units 2, 3 and 4 had a relatively high yield, averaging more than 90%.

3.3. PM composition

The PM composition was a strong function of whether the PM was generated under non-regeneration or regeneration conditions. The non-regeneration PM was dominated by EC (~90%), with small amounts of OC (~9%) and trace amounts of sulfur (Johnson et al., 2010). For these measurements, EC levels were well above the detection limits, while the OC and sulfur measurements were near the detection limits. Additional analysis was performed by SwRI using a direct filter injection system for a gas chromatograph (US Patent # 5109710). During this analysis, SwRI analyzed five selected MEL Teflon filters and 5 from SwRI (from the MA model development work). The results showed that the MEL filters were between 10 and 20% OC, SwRI steady state filters were 32%–57% OC, and the SwRI transient filters were between 14% and 16% OC (Khalek et al., 2010). These results suggest that the OC fraction for the in-use transient testing may be on the same order as suggested by UCR's results. It also suggests that the steady state testing may have a different composition than the transient and in-use testing results.

The regeneration filter samples collected were typically composed of predominately nucleated hydrated sulfate particles ($H_2SO_4.6H_2O$), as shown by others (Swanson et al., 2009). A separate analysis of EC, OC and sulfur measurements was performed for selected regeneration filters. These results showed only trace amounts of EC and OC, and a dominate amount of sulfur (~98%). This suggests that nearly all the PM mass was hydrated sulfate particles for the regeneration cases.

3.4. Particle size distribution (PSD)

Particle number (CPC 3760) and size distributions (fSMPS) were measured throughout the testing. The PSDs for typical non-regeneration and regeneration cases are provided in the Fig. 4. The size distributions showed an average number diameter of 64 nm for the non-regeneration cases and 13 nm for the regeneration cases. Higher particle number concentrations (~5 times) were observed during the regeneration cases in comparison to non-regeneration cases. The combination of the regeneration particle composition being dominated by sulfate and number averaged

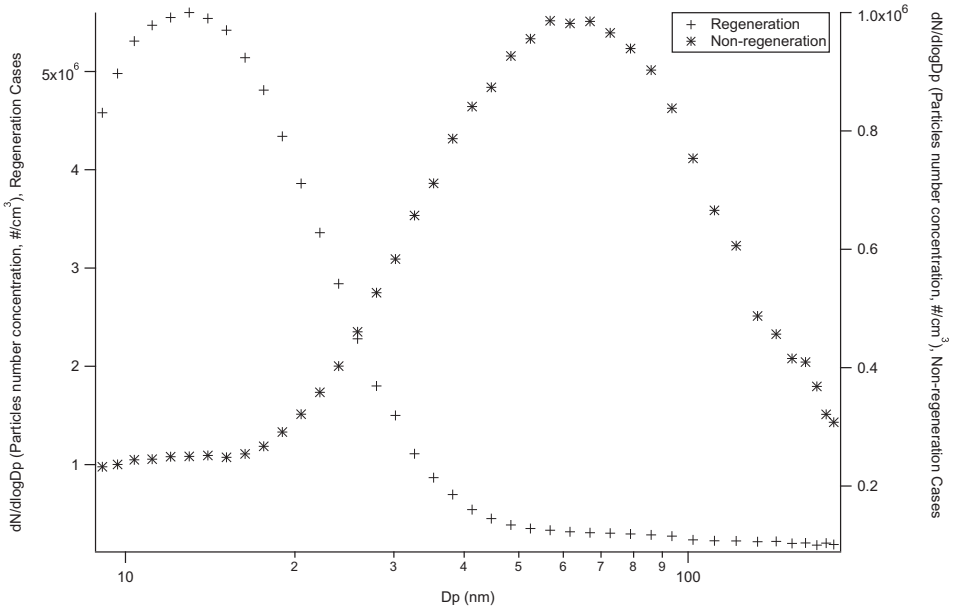

Fig. 4. PM number size distribution (dN/dlogDp) for a typical non-regeneration and regeneration conditions. Note that the *x*-axis is on logarithmic scale.

diameter of 13 nm suggests the particles contributing to the PM mass were formed predominantly from the conversion of SO_2 to SO_3 over the catalytic surfaces of the DPF, as discussed previously (Johnson et al., 2011; Swanson et al., 2009). These nanoparticles represent a homogeneous nucleation that formed during simultaneous dilution and condensation inside the CVS tunnel. Thus, it is possible that the PEMS and MEL may see different particles diameters due to their different locations, but typically particle formation with similar dilution ratios and temperatures should form similar mass levels. The correlation between the reference and the PEMS and INST was poorest for the regeneration tests compared to the non-regeneration tests. It is unclear, however, if the reason for the poor correlation for all PEMS and INST is due to the composition, particle size, or both, or other instrument issues. Small particle size probably contributed to a low signal response for several PM-PEMS instruments. Specifically, small particles do not scatter light well, thus affecting INST4(LS), and small particles affect the ability for INST5(EM + A) to use its assumption of a log normal distribution being centered at 100 nm for its impactor electrometers.

4. Conclusions

This research provides the latest evaluation of PM-PEMS performance, accuracy, and precision compared to the gravimetric reference method. The research from this study shows current PM-PEMS typically underreport the PM emissions compared to the reference method, with the exception of the PEMS3(PA + F) which incorporated a gravimetric filter. Both PEMS2(QCM) and PEMS3(PA) showed very similar unit-to-unit performance with PEMS3(PA) being precise. The changes in performance between older and newer versions of the same PEMS is also of interest. The variability between different versions was low for some PM-PEMS, but for others there was about a factor of 5 differences between different versions. The large variability between newer and older versions of the same PM-PEMS for some PEMS suggests these PEMS are very sensitive to parameters changes and the version number of a PEMS should be included as part of future publications.

Regenerations continue to be difficult for PM-PEMS to quantify. During this and a previous in-use study PM-PEMS were only able to quantify about 20% of the mass of the gravimetric reference method. INST5(EM + A) technology showed the best regeneration correlation during both studies. The filter-based PEMS3(PA + F) system was unable to correlate well with the MEL when the PM was composed of hydrated sulfate nanoparticles, but it has the potential to correlate with organic dominated PM. Micro-dilution may be the root cause for the low correlation for the sulfuric acid nanoparticles for the PM-PEMS. More analysis and evaluation is needed to fully characterize the non-soot dominated PM.

INST4(LS) and INST5(EM + A) correlation slope decreased between this study and the previous study. The lower slope could be due to a measurement issue at lower concentrations for the current study. This suggests these PEMS would significantly underreport at the levels of a properly functioning DPF at the sub 1 mg $hp^{-1}h^{-1}$. It is also known from internal work that at the sub 1 mg $hp^{-1}h^{-1}$ emission level, the reference method is at the detection limits of its measurement capability. At this level, INST4(LS) is below its detection limits, but INST(EM + A) still has a fairly strong measurement signal. Since INST5(EM + A) has a strong signal and the reference method is at its detection limit, INST5(EM + A) may be the only suitable measurement tool to help characterize sub 1 mg $hp^{-1}h^{-1}$ emissions such as during DPF regeneration.

In general, this research has shown that PM-PEMS have continued to evolve, and have improved in their correlation with the gravimetric filter for some PEMS, but not all. Overall, some PM-PEMS are suitable to quantify DPF failures at the OBD-HD thresholds to within 10%. Other PM-PEMS could significantly under or over report these PM emissions depending on what versions of the PM-PEMS is used. This study also uncovered some issues with firmware, hardware, and post processing upgrades that can have a significant impact on the reported emissions. The implications from this study suggest that not all PM-PEMS are at the same level of development maturity with respect to correlations with gravimetric filter mass and that new PM-PEMS need to be carefully evaluated before they are widely adopted for emission inventory or regulatory purposes. The inclusion of the gravimetric filter has shown to improve the PM-PEMS performance, but these benefits are not equal for all PM compositions and additional studies are needed.

Acknowledgments

The California Air Resources Board (CARB), US EPA, and Engine Manufacturer's Association (EMA) funded this work. The authors acknowledge the support of the Measurement Allowance Steering Committee (MASC) for assistance in developing and carrying out this program. The authors acknowledge Sensors Inc., and AVL for providing the PM-PEMS as an in-kind contributions. We also acknowledge Cummins for their engineering assistance on controlling the regenerations and managing DPF soot levels. Lastly, we acknowledge Mr. Donald Pacocha and Mr. Joe Valdez, University of California at Riverside, for their contribution in setting up and executing this field project, the data collection and quality control.

References

Baron, P.A., Willeke, K., 2001. Aerosol Measurement: Principles, Techniques, and Applications. John Wiley, New York.
Bell, A., Phil, G., 1881. Mag. J. Sci. XI, 510–528.
Booker, D.R., Giannelli, R.A., Hu, J., 2007. Road Test of an On-Board Particulate Matter Mass Measurement System. SAE 2007-01-1116.
CARB, 2010. California Air Resources Board, Final Regulation 1971.1 (e) Monitoring Requirements for Diesel/Compression-Ignition Engines (8) Particulate Matter (PM) Filter Monitoring (8.2)(8.2.1) Filtering Performance.
CFR. Code of Federal References, 2010. Protection of the Environment. Title 40. Section 86 and 89.
Clerc, J.C., Johnson, J.H., October 18, 1982. A Computer Heat Transfer and Hydrocarbon Adsorption Model for Predicting Diesel Particulate Emissions in Dilution Tunnels. SAE 821218.
Cocker, D.R., Shah, S.D., Johnson, K.C., Miller, J.W., Norbeck, J.M., 2004a. Development and application of a mobile laboratory for measuring emissions from diesel engines. 1. Regulated gaseous emissions. Environ. Sci. Technol. 38, 2182.
Cocker, D.R., Shah, S.D., Johnson, K.C., Zhu, X., Miller, J.W., Norbeck, J.M., 2004b. Development and application of a mobile laboratory for measuring emissions from diesel engines. 2. Sampling and toxics and particulate matter. Environ. Sci. Technol. 38, 6809.
Durbin, T.D., Johnson, K.C., Cocker, D.R., Miller, J.W., 2007. Evaluation and comparison of portable emission measurement systems and federal reference methods for emissions from a back-up generator and a diesel truck operated on a chassis dynamometer. Environ. Sci. Technol. 41, 6199–6204. http://eprints.cert.ucr.edu/448/.
Fountoukis, C., Nenes, A., 2007. ISORROPIA II: a computationally efficient aerosol thermodynamic equilibrium model for K^+–Ca^{2+}–Mg^{2+}–NH_4^+–SO_4^{2-}–NO_3^-–Cl^-–H_2O Aerosols. Atmos. Chem. Phys. 7, 4639–4659.
Harren, Frans J.M., Cotti, Gina, Oomens, Jos, te Lintel Hekkert, Sacco, 2000. In: Meyers, R.A. (Ed.), Photoacoustic Spectroscopy in Trace Gas Monitoring, Encyclopedia of Analytical Chemistry. John Wiley & Sons Ltd, Chichester, pp. 2203–2226.
Hinds, W.C., 1998. Aerosol Technology. John Wiley, New York.
ISORROPIA, 2009, http://nenes.eas.gatech.edu/ISORROPIA.
Johnson, K.C., Durbin, T.D., Cocker III, D.R., Miller, W.J., Bishnu, D.K., Maldonado, H., Moynahan, N., Ensfield, C., Laroo, C.A., 2009. On-road comparison of a portable emission measurement system with a mobile reference laboratory for a heavy duty diesel vehicle. Atmos. Environ. http://eprints.cert.ucr.edu/338/.
Johnson, K.C., Durbin, T.D., Jung, H., Cocker III, D.R., Khan, M.Y., November 2010. Validation Testing for the PM-PEMS Measurement Allowance Program. In: Final Report by the University of California Riverside for the California Air Resources Board under Contract No. 07-620. http://eprints.cert.ucr.edu/505/.
Johnson, K.C., Durbin, T.D., Jung, H., Cocker, D.R., Bishnu, D., Giannelli, R., 2011. Environ. Sci. Technol. 45 (14), 6073–6079.

Khalek, I.A., Bougher, T.L., Mason, R.L., Buckingham, J.P., 2010. PM-PEMS Measurement Allowance Determination, Final Report by Southwest Research Institute for the Heavy Duty In-Use Testing Steering Committee. SwRI Project 03.14956.12, June.

Lehmann, U., Niemela, V., Morh, M., 2004. New methods for time resolved diesel engine exhaust particle mass measurements. Environ. Sci. Technol. 38, 5704–5711.

Maricq, M.M., Xu, N., Chase, R.E., 2006. Measuring particulate mass emissions with electrical low pressure impactor. Aerosol. Sci. Technol. 40, 68–79.

Matter, U., Siegmann, H.C., Burtscher, H., 1999. Dynamic field measurements of submicron particles from diesel engines. Environ. Sci. Technol. 33, 1946–1952.

Mohr, M., Lehmann, U., Rutter, J., 2005. Comparison of mass-based and non-Mass-Based particle measurement systems for Ultra-low emissions from Automotive Sources. Environ. Sci. Technol. 39, 2229–2238.

Nenes, A., Pilinis, C., Pandis, S.N., 1998. ISORROPIA: a new thermodynamic model for multiphase multicomponent inorganic Aerosols. Aquat. Geochem. 4, 123–152.

NIOSH, 1996. NIOSH Manual of Analytical Methods. National Institute of Occupational Safety and Health, Cincinnati, OH.

Podsiadlik, D.H., Chase, R.E., Lewis, D., Spears, M., 2003. Phase-based Teom Measurements Compared with Traditional Filters for Diesel PM. SAE 2003-01-0783.

Ristimaki, J., Virtanen, A., Marjamaki, M., Rostedt, A., Keskinen, J., 2002. On-line measurement of size distribution and effective density of submicron particles. J. Aerosol. Sci. 33, 1541–1557.

Schindler, W., Haisch, C., Beck, A.H., Niessner, R., Jacob, E., Rothe, D., 2004. A Photoacoustic Sensor System for Time Resolved Quantification of Diesel Soot Emissions. SAE 2004-10-0968.

Shah, S.D., Cocker, D., 2005. A fast scanning mobility particle spectrometer for monitoring transient particle size distributions. J. Aerosol. Sci. 39, 519–526.

Swanson, J., Kittelson, D., Watts, W., Gladis, D., Twigg, M., 2009. Influence of storage and release on particle emissions from new and used CRTs. Atmos. Environ. 43, 3998–4004.

Traver, M.L., May 2002. Inter-laboratory Crosscheck of Heavy Duty Vehicles Chassis Dynamometers. CRC Project No. E-55–1.

Witze, P.O., Maricq, M.M., Chase, R.E., Podsiadlik, D.H., Xu, N., 2004. Time-resolved measurements of exhaust PM for FTP-75: Comparison of LII, ELPI, and TEOM Techniques. SAE 2004-01-0964.